



ASME Accepted Manuscript Repository

Institutional Repository Cover Sheet

Cranfield Collection of E-Research - CERES

ASME Paper

Title: Thrust rebalance to extend engine time on-wing with consideration of engine degradation and
creep life consumption

Authors: Rafael da Mota Chiavegatto, Yiguang Li

ASME Journal

Title: Journal of Engineering for Gas Turbines and Power

Volume/Issue: Volume 146, Issue 9

Date of Publication (VOR* Online): 18 October 2023

ASME Digital Collection <https://asmedigitalcollection.asme.org/gasturbinespower/article/doi/10.1115/1.4063791/1169520/Thrust-Rebalance-to-Extend-Engine-Time-On-Wing>

DOI: <https://doi.org/10.1115/1.4063791>

*VOR (version of record)

THRUST REBALANCE TO EXTEND ENGINE TIME ON-WING WITH CONSIDERATION OF ENGINE DEGRADATION AND CREEP LIFE CONSUMPTION

Rafael Chiavegatto

Yi-Guang Li

School of Aerospace, Transport and Manufacturing,
Cranfield University, Cranfield, Bedford MK43 0AL, UK

ABSTRACT

Over the years, airlines have consistently attempted to lower their operational costs and improve aircraft availability by applying various technologies. Engine maintenance expenses are one of the most substantial costs for aircraft operations, accounting for around 30% of overall aircraft operational costs. So, maximizing aircraft time between overhaul is crucial to lowering the costs. The engine time on-wing is often limited due to the expiration of Life Limiting Parts, performance deterioration, etc.

This paper presents a novel method of rebalancing the thrust of engines of an aircraft to maximize the time between overhaul of the aircraft considering the performance degradation and creep life consumption of the engines. The method is applied to a model aircraft fitted with two model engines similar to GE90 115B to test the feasibility of the method with one engine degraded and the other engine undegraded. The obtained results demonstrate that for the aircraft flying between London and Toronto with 5,000 nominal flight cycles given to the engines, the time on-wing of the degraded engine could drop from 5,000 to 2,460 flight days due to its HP turbine degradation (1% efficiency degradation 3% flow capacity degradation), causing the same level of drop of time between overhaul of the aircraft. The time on-wing of the degraded engine could increase from 2,460 flight days without thrust rebalance to 3,410 flight days with thrust rebalance, i. e. around 38.6% potential improvement for the time between overhaul of the aircraft at the expenses of increased creep life consumption rate of the clean engine. The proposed method could be applied to other aircraft and engines.

Keywords: Gas Turbine, Engine, Thrust Rebalance, Creep Life, Performance Degradation

NOMENCLATURE

| | |
|--------------------|--|
| A | Cross sectional area (m^2) |
| BM | Bending moment |
| C_p | Specific heat ($J/kg/K$) |
| CF | Creep factor |
| CL | Creep life |
| ECF | Equivalent creep factor |
| h | Height (m) |
| HP | High Pressure |
| I | Second moment of area |
| LMP | Larson-Miller Parameter |
| LP | Low Pressure |
| m | Mass (kg) |
| NT | Net thrust (N) |
| P | Pressure (kPa) |
| PCN | Fan shaft relative rotational speed |
| \dot{Q} | Heat rate (kW) |
| SFC | Specific Fuel Consumption ($g/s/kN$) |
| $RTDF$ | Radial Temperature Distribution Factor |
| t_f | Time to failure (hours) |
| T | Temperature (K) |
| $TBF (\lambda)$ | Thrust Balance Factor |
| TET | Turbine Entry Temperature (K) |
| σ | Stress (N/m^2) |
| ω | angular speed of rotation (rad/s) |
| ε_{ff} | overall cooling effectiveness |

Subscripts

| | |
|------------|-------------------|
| <i>b</i> | Blade |
| <i>bl</i> | Baseline |
| <i>c</i> | Clean |
| <i>CF</i> | Centrifugal force |
| <i>d</i> | Degraded |
| <i>g</i> | Gas |
| <i>in</i> | Inlet |
| <i>out</i> | Outlet |

Superscripts

| | |
|------------|----------------|
| <i>Tot</i> | Total |
| <i>BM</i> | Bending Moment |

1. INTRODUCTION

Most civil passenger aircraft are powered by multiple gas turbine engines and normally all engines equally contribute thrust to meet the total thrust requirement. During lifetime of operation, engine performance will degrade due to engine degradations, such as fouling, erosion, corrosion, foreign object damage, etc. To produce the same level of thrust, the degraded engines have to work harder compared with the clean or undegraded engines and consequently the degraded engines have to experience higher turbine entry temperature and higher shaft rotational speeds resulting in higher thermal and mechanical stresses and shorter life. Therefore, the degraded engines may have shorter time on-wing and dominate the maintenance activities of the aircraft.

Creep is one of the most common failure modes of gas turbine engines. The high-pressure (HP) turbine blades are one of the creep life-critical components within gas turbine engines due to their experience of both the highest thermal and mechanical stresses. Several studies have been conducted in the past to establish the influence of various operation scenarios on engine creep life.

Naeem et al. [1-3] evaluated the impact of engine degradation and varying ambient temperature on HP turbine blades' creep life of aircraft engines. Tinga et al. [4] assessed the influence of engine deterioration on the creep life of the HP turbine blades of a turbofan engine similar to F100-PW-220. Liu et al. [5-6] evaluated the influence of hot gas temperature, engine shaft speed, cooling flow

temperature, and cooling hole diameter on the creep life of HP turbine blades of a gas turbine engine. A combined response surface Monte Carlo method was used by Wallace et al. [7] to look at the influence of gas temperature, external heat transfer coefficient, creep constant variation parameter, and cooling hole friction on the creep life of HP turbine blades. Abdul Ghafir et al. [8] introduced a Creep Factor concept to assess the relative creep life consumption of a turboshaft engine. Saturday, et al. [9] extend the concept of Creep Factor to an Equivalent Creep Factor and demonstrated its application to an industrial gas turbine engine operating for a period of time in the assessment of the relative creep life consumption using the field data of the engine.

In aviation industry, thrust control of aircraft engines in certain scenarios has been conducted for either extending engine life or protecting the engines from damages. For example, thrust derating of aircraft engines at take-off and climbing is one of them and James and O'Dell [10] has studied it and shown that such practice can reduce engine life consumption, reduce engine degradations and considerably save maintenance costs with the expenses of a small increase in fuel consumption and flight time. Research on thrust rating was done by Atif Shafi [11] and the impact of thrust rating on engine time on-wing was analyzed. Another thrust control is the flat rating for aircraft engines during high ambient temperature to protect the engines from overheating. Only in an exceptional circumstance where an engine failure happens, the remaining engine(s) on the same aircraft must produce additional thrust to maintain safe flight to the nearest airport. However, under normal practices all engines installed on an aircraft produce the same level of thrust even in thrust derating and flat rating conditions. There is no published research so far to discuss asymmetric thrust balancing. The current aircraft safety regulations [12] have no mentions about such type of practice.

In this study, a novel thrust rebalance method is introduced for a twin-engine aircraft to maximize the time between overhaul of the aircraft when one of the engines is degraded. The detailed methodology of the thrust rebalance method is given, and the application of the method is demonstrated with a model aircraft similar to Boeing 777-300ER powered by two model engines similar to GE90 turbofan engines.

2. METHODOLOGY

2.1 Thrust Rebalance Method

For a civil passenger aircraft powered by two engines, both engines may produce equal thrust to share the total thrust requirement. Consequently, both engines would have the same load, experience the same mechanical and thermal stresses and therefore the life would

be consumed at a similar rate. This is beneficial to the aircraft maintenance schedule as the time on-wing for both engines is more or less the same.

However, at the situation where the health of the two engines is different, such as one engine being healthy or clean and the other being degraded, the degraded engine must work harder than the healthy engine in order to produce the required thrust. Consequently, the degraded engine has to run at higher shaft rotational speed and higher turbine entry temperature, and therefore result in quicker life consumption. This is not a good situation for aircraft maintenance as the degraded engine may have shorter time on-wing and therefore result in shorten time between overhaul of the aircraft.

To maximize the time between overhaul for the aircraft in this situation, the operation of the two engines may be adjusted by shifting a small proportion of thrust from the degraded engine to the clean engine as shown in Fig. 1 while the total thrust required by the aircraft is kept unchanged. In other words, the clean engine may share relatively more thrust generation than the degraded engine with the objective of keeping both engines having the same time on-wing, which is referred to as thrust rebalancing.

Such an approach can only be used when both engines are working but have different levels of acceptable degradations. In an engine out scenario, the remaining engine has to provide minimum thrust required by aircraft regardless of its degradation for continued flight to a nearest airport for a safe landing.

To quantify the amount of shifted thrust, a Thrust Balance Factor (TBF) λ has been introduced and is defined by Eq. (1).

$$\lambda = \frac{\Delta NT}{NT_{bl}} \quad (1)$$

Where NT_{bl} is the net thrust of an engine at its baseline condition, and ΔNT is the amount of thrust shifted from the baseline condition. For a twin-engine aircraft, the thrust balance factors for the two engines may be different when the health of the two engines is different. It is assumed that at the baseline condition, the power control parameter, i. e. the engine handle parameter is kept at the same value no matter the engine is clean or degraded.

If the thrust balance factor for the clean engine (λ_c) is controlled, the thrust balance factor of the degraded engine (λ_d) is then mainly determined by both the thrust rebalance of the clean engine and the level of degradation of the degraded engine. To keep the

same total thrust required by the aircraft, the thrust balance factor of the degraded engine may be represented as a function of that of the clean engine represented by Eq. (2); the process of obtaining such a relationship is given in Appendix A.

$$\lambda_d = \frac{NT_{c,bl}}{NT_{d,bl}} \cdot (1 - \lambda_c) - 1 \quad (2)$$

where $NT_{c,bl}$ and $NT_{d,bl}$ are the net thrust of the clean and the degraded engines, respectively. Bear in mind that $NT_{d,bl}$ is determined by the degradation of the degraded engine.

Fig. 2 shows how performance parameters of both the clean and the degraded engines vary with TBF of the clean engine and discussions are given in the following possible scenarios:

- (1) At the baseline condition ($\lambda_c = 0$) where both engines keep the same power handle value, the net thrust produced by the clean engine is noted at Point A while the degraded engine may produce less net thrust at Point D shown in Fig. 2(a) with a slightly higher TET at Point M in Fig. 2(b). As the aircraft total thrust demand is unchanged, the degraded engine has to boost its thrust from Point D to Point A. Consequently, the degraded engine would have to work at an even higher turbine entry temperature indicated at Point N shown in Fig. 2(b) to recover the loss of the net thrust, resulting in a significant rise of the creep life consumption rate of the engine as shown in the drop of ECF from Point R to Point T in Fig. 2(c), which may result in a positive λ_d indicated by Point H in Fig. 2(a).
- (2) When the thrust rebalance is applied to both the clean and degraded engines, the net thrust and TET of the clean engines increase while the net thrust and TET of the degraded engine decrease. This will result in the decrease of ECF for the clean engine and the increase of ECF for the degraded engine. At the condition indicated at Points F and G shown in Fig. 2(a) where $\lambda_c = 1 - \frac{NT_{d,bl}}{NT_{c,bl}}$, the net thrust of the degraded engine becomes equal to its net thrust at the baseline condition at Point D. Consequently, the thrust balance factor of the degraded engine becomes $\lambda_d = 0$, indicating a turning point of TBF of the degraded engine from positive to negative values at Point J.
- (3) When the thrust rebalance increases further and $\lambda_c > 1 - \frac{NT_{d,bl}}{NT_{c,bl}}$ shown in the area around Points B, C and I in Fig. 2(a) where the TBF of the degraded engine will take a negative value, the net thrust of the clean engine will continue to increase while the net thrust of the degraded engine will continue to reduce. At the same time, TET of the clean engine will continue to increase while TET of the degraded engine will continue to decrease as shown in Fig 2(b). In other words, the degraded engine would be able to

reduce its life consumption rate at the expenses of the increase of the life consumption rate of the clean engine. This is shown with an increase of ECF of the degraded engine at Point S and the decrease of ECF of the clean engine indicated at Point Q in Fig. 2(c).

- (4) During the process of increasing the thrust rebalance, Point U in Fig. 2(c) may be found at a certain TBF where ECF of both engines reach the same value, which indicates that the creep life of both engines is consumed at the same rate. This could be the best level of thrust rebalance to make both the clean and the degraded engine staying on-wing for the same period of time before consuming all of their flight cycles.

Based on the above, it shows that by applying the engine thrust rebalance, the shortage of life of the degraded engine can be compensated by sacrificing the life of the clean engine and the time between overhaul of the aircraft can be potentially maximized.

The concept of life for an aircraft engine can be broad and life critical components can be many. To demonstrate the thrust rebalance method, it is assumed in this study that the engines are used for a long-haul civil passenger aircraft, so creep life consumption plays a dominant role in engine life consumption and therefore is only considered in this study. Other types of life consumptions, such as low cycle fatigue life and oxidation life are not considered. The critical component in aircraft engines for creep life is the high-pressure turbine rotor blades that experience both the highest mechanical stress due to highest centrifugal load and the highest thermal stress due to highest surrounding gas temperature. Therefore, the creep life consumption of the HP turbine rotor blades of the aircraft engines is the focus of the thrust rebalance study.

Figure 3 depicts the calculation flow chart of the thrust rebalance method, which outlines how the thrust rebalance can be applied to the two gas turbine engines installed on the same aircraft:

- Ambient conditions, flight mission profile and blade geometry and material data are provided as input information.
- The gas turbine performance model calculates the performance of both the clean and the degraded engines and provide the boundary conditions for the blade thermal and stress models.
- The blade thermal model calculates the heat transfer between the blades and gas, and the material temperature of the HP turbine blades.
- A stress model calculates the mechanical stress of the HP turbine rotor blades.
- A creep lifing model calculates the Equivalent Creep Factors of the HP turbine blades for the flight cycles
- The thrust rebalance model provides an iterative process to find the thrust balance factor that could make the Equivalent Creep Factor (ECF) of both engines the same.

Once the ECF of both the clean and the degraded engines become equal, it means that the two engines could have the same remaining life or flight cycles, i. e. the same on-wing time before the next overhaul.

The following sections provide some details of the individual models to assist the understanding of the thrust rebalance method.

2.2 Gas Turbine Performance Model

The thermodynamic performance of aircraft engines is simulated with fundamental thermodynamics and empirical engine component maps. The details of the simulation methods can be found in [13]. Cranfield software Pythia [14-15] on gas turbine performance, gas path diagnostics and life consumption analysis is used for this research.

2.3 Blade Stress Model

The blade stress model [9] estimates mechanical stress at various positions along a HP turbine blade's span and finds the maximum stress on the blade. The stress model includes two significant stress components, one is the centrifugal stress, and the other is bending momentum stress.

The centrifugal stress at each node i along blade height may be given by Eq. (3).

$$\sigma_{CF,i} = \frac{m_{b,i} * \omega^2 * h_i}{A_i} \quad (3)$$

where $m_{b,i}$ is the mass of the section i , ω the angular speed of rotation, h_i the distance from the centre of gravity of the section to the turbine axis of rotation, and A_i the cross-sectional area of the blade at node i .

Fig. 4 illustrates the orientations of the blade cross section. The specific bending moment stresses at the blade section i may be obtained using Eq. (4).

$$\sigma_i^{BM} = \frac{BM_{XX,i} * Y_i}{I_{XX,i}} + \frac{BM_{YY,i} * X_i}{I_{YY,i}} \quad (4)$$

where , $BM_{XX,i}$ is the axial bending moment, $BM_{YY,i}$ the tangential bending moment I_{XX} the second moment of area about the blade axial direction, I_{YY} the second moment of area about the blade tangential direction, and X_i and Y_i the distances between the centre of gravity and the respective locations on the blade section.

Therefore, the total stress at the root of each blade segment is given by Eq. (5)

$$\sigma_i^{Tot} = \sigma_{CF,i} + \sigma_i^{BM} \quad (5)$$

The maximum stress σ at each section's root is the total of the surface stresses, given by Eq. (6)

$$\sigma_{max,i} = \max(\sigma_i^{Tot}) \quad (6)$$

More details of the blade stress model can be found in [9].

2.4 Blade Thermal model

A blade thermal model is created based on total energy continuity to estimate the material temperature distribution throughout the blade span. It considers heat transfer between the cooling air from the upstream compressor flowing through a single pass cooling channel inside the blade as shown in Fig. 5 and the mainstream hot gas outside traversing the blade assuming that only convection is considered. For simplicity, the blade is divided into eight equal parts along the span and nine nodes are used to represent the radial metal temperature distribution. The mainstream radial gas temperature distribution is assumed to be the one shown in Fig. 5 where the maximum gas temperature occurs at 62.5% of blade height, the minimum gas temperature occur at both the blade root and blade tip and the temperature is linearly distributed considering that the cooling is the best around mid-blade height. Therefore, the nodal temperatures of the gas can be obtained by Eq. (7).

$$T_{g,i} = \begin{cases} T_{g,min} + (T_{g,max} - T_{g,min}) \cdot \frac{i-1}{5}, & 1 \leq i \leq 6 \\ T_{g,min} + (T_{g,max} - T_{g,min}) \cdot \frac{9-i}{3}, & 6 < i \leq 9 \end{cases} \quad (7)$$

The maximum radial temperature at the turbine inlet is determined by radial temperature distribution factor (RTDF), as shown by Eq. (8) and the minimum radial temperature can be obtained by Eq. (9).

$$T_{g,max} = T_{g,mean} + RTDF \cdot (T_{g,mean} - T_{com,in}) \quad (8)$$

$$T_{g,min} = \frac{9T_{g,mean} - 4T_{g,max}}{5} \quad (9)$$

where $T_{g,mean}$ is the turbine inlet mean gas temperature and $T_{com,in}$ the combustor inlet mean air temperature; both can be obtained from engine performance model.

The blade metal temperatures are determined using convective cooling theory. In other words, the energy input to the whole blade from the hot gas, \dot{Q}_{in} equals the energy removed by the cooling flow, \dot{Q}_{out} , Eqs. (10)-(12).

$$\dot{Q}_{in} = \dot{Q}_{out} \quad (10)$$

$$\dot{Q}_{in} = h_g B_p h_b (T_g - T_b) \quad (11)$$

$$\dot{Q}_{out} = \dot{m}_c C_p (T_{c,ex} - T_{c,in}) \quad (12)$$

where h_g is the external heat transfer coefficient, B_p the perimeter of the blade, h_b the blade height, T_g the gas temperature, T_b the blade metal temperature, C_p the specific heat capacity of the cooling air, \dot{m}_c the coolant mass flow rate, $T_{c,in}$ the coolant inlet temperature, and $T_{c,ex}$ the coolant exit temperature.

For each of the blade section i , the metal mean temperature may be estimated by Eq. (13).

$$T_{b,i} = T_{g,i} - \varepsilon_{ff}(T_{g,i} - T_{c,in,i}) \quad (13)$$

where ε_{ff} is the overall cooling effectiveness and assumed to be a constant across the blade. More details of the blade thermal model can be found in [9].

2.5 Blade Lifting Model

Lifting is the process of forecasting the lifetime ahead of each engine components. Creep is one of the major causes of damage and defined as a material's gradual plastic deformation over a period of time due to high temperature and mechanical stress. A long-haul civil aircraft may spend most of its flight hours in cruise mode, and creep become a critical failure mode on engine turbine blades.

Different techniques of calculating the creep life of critical components of gas turbine engines have been published [16–18]. Among these methods, the Larson-Miller Parameter (LMP) method represented by Eq. (15) is preferable in this study due to its simplicity and broad applicability [14]

$$t_f = 10^{\left(\frac{LMP}{T_b} - C\right)} \quad (14)$$

where t_f is time to failure in hours, T_b the blade material temperature in Kelvin, C material constant and LMP the Larson-Miller Parameter.

The reliability of Larson-Miller Parameter method relies on the accuracy of the predicted blade metal temperature, selection of the constant C , and the LMP. In this study, the constant C is chosen to be 20 owing to its applicability in most technical applications [9]. The LMP is determined by the mechanical stress estimated by a stress model described in Section 2.3. The blade material temperature is calculated by the blade thermal model described in Section 2.4.

Due to the fact that the estimated creep life for the engines using the Larson-Millar Parameter method may have significant errors due to many uncertain factors associated with blade geometry, material properties, flow conditions, estimated blade material temperature, etc., Creep Factor (CF) [8] is used to represent the relative creep life consumption rate of the engine at any time moment against that at a user-specified reference condition and Equivalent Creep Factor (ECF) [9] is used to describe the relative creep life

consumption of a whole mission against that at the reference condition. The advantage of using CF and ECF is to assess the impact of varying ambient and operating conditions and flight missions on the creep life consumption relative to that at the reference condition so the absolute errors in the predictions of blade creep life become less important.

An actual flight mission profile for an aircraft engine may be complicated. However, it can be discretized into many small constant processes schematically shown in Fig. 6 for convenient calculations.

Creep Factor [8] is defined as the ratio between the creep life at any condition and the creep life at a user-specified reference condition as shown by Eq. (15).

$$CF = \frac{CL}{CL_{Ref}} \quad (15)$$

where CL is the calculated creep life of the engine at any operating condition, and CL_{Ref} is the calculated creep life at the reference condition; both are predicted by the Larson-Miller method.

For a complete flight mission, Equivalent Creep Factor (ECF) [9] is defined by Eq. (16)

$$ECF = \frac{\left(\frac{\sum_{i=1}^m T_i}{\sum_{i=1}^m CL_i} \right)}{CL_{Ref}} \quad (16)$$

where T is the time of a flight time span and m is the total number of time spans of the entire flight mission. Depending on the value of CF or ECF, they indicate the relative creep life consumption rate. For example, if

- CF or $ECF < 1$, the engine life is consumed faster than that at the reference condition
- CF or $ECF = 1$, the engine life is consumed at the same rate as that at the reference condition
- CF or $ECF > 1$, the engine life is consumed slower than that at the reference condition

The assessment of ECF in the analysis of the thrust rebalance impact would allow the aircraft operators to control the life consumption of the engines for better maintenance practice.

3 DEMONSTRATION OF APPLICATION

A case study is demonstrated in this section to show the benefits of applying the thrust rebalance method to a model civil passenger aircraft, similar to Boeing 777-300ER powered by two model engines, similar to GE90-115B.

3.1 Model Engine

The model engine, similar to GE90-115B [19] as shown in Fig. 7 is a two-shaft, high bypass ratio civil turbofan engine with a one-stage fan and a four-stage LP compressor (booster) driven by a six-stage LP turbine, a nine-stage HP compressor driven by a two-stage HP turbine and a combustor. The performance specification of the model engine is shown in Table 1.

The thermodynamic performance model for the model engine was set up with the Cranfield gas turbine performance and diagnostics software Pythia [14] and the model configuration is shown in Fig. 8. The fan shaft rotational speed PCN is chosen as the engine power control parameter (i. e. handle parameter) to control the engine operating conditions at off-design and degraded conditions.

3.2 Flight Mission

It is assumed that two of the same type of engines are installed on the aircraft flying between London and Toronto,. They take one flight per day every day and each flight takes about 9 hours. The engine flight mission profile is shown in Fig. 9 where the altitude, Mach number and the engine handle parameter PCN varying with the flight time are shown.

3.3 Engine Degradation Profile

It is assumed that one engine is clean (un-degraded) and the other is degraded. In this study, it is assumed that the degraded engine has a HP turbine degradation, with the efficiency degraded by -1% and the flow capacity degraded by -3%. For simplicity, it is assumed that such degradation scenario is unchanged during operations, and no other components are degraded.

3.4 Thrust Rebalance and Lifting Analysis

The degraded engine runs less efficiently compared with the clean engine. Therefore, the degraded engine has to work harder to keep the same net thrust by increasing engine fan shaft speed PCN, which would lead to an increased TET and a higher creep life consumption rate. Figs. 10 and 11 shows the amount of increase of PCN and TET of the degraded engine relative to the clean engine at different flight sections of the flight mission. It can be seen that the engine power handle PCN has to increase up to around 0.75% and TET has to rise up to around 8K in order to produce that same amount of thrust as that of the clean engine.

Figure 12 depicts the changes in creep factors of both the clean and the degraded engines at all flight sections as a function of the thrust balance factor (TBF) of the clean engine, where Fig. 12(a) shows the whole flight time while Fig. 12(b) zooms on the first 20 minutes. It can be seen in Fig. 12(b) that the low CF happens in the first 13 minutes after taking off, and the CF of the degraded engine is lower than that of the clean engine. It means that the creep life of both the clean and the degraded engines consumed faster in the first

13 minutes than in other flight sections and the degraded engine consumed its creep life even faster than the clean engine. Fig. 12 also shows ECF of the whole flight mission, with the ECF of the clean engine being around 250 while the ECF of the degraded engine being around 195, indicating that the degraded engine is consuming its creep life roughly 22% faster than the clean engine.

To assess the impact of the thrust rebalance method on the two engines, it is assumed that both engines are given 5,000 flight cycles at the beginning of the operation and the aircraft takes one flight per day.

When the thrust rebalance is applied to the two engines for the flight mission, the performance and the creep life consumption of the engines are changing. Take an example at the cruise flight condition, as the degraded engine has to work harder to produce the same amount of net thrust as that of the clean engine without thrust rebalance as shown in Fig. 13, its fan shaft PCN increases to 0.906, TET rises to 1,467K, and TBF takes the value of 2.63% initially as shown in Figs. 14 to 16. With the increase of TBF of the clean engine, the net thrust of the clean engine increases and the net thrust of the degraded engine decreases, as shown in Fig. 13, while the total net thrust of both engines are kept unchanged. This is achieved by increasing the power handle PCN of the clean engine and decreasing the PCN of the degraded engine, as shown in Fig. 14. Consequently, the TET of the clean engine increases while the TET of the degraded engine decreases, as shown in Fig. 15. With the TBF of the clean engine increases from 0% to 4%, the TBF of the degraded engine decreases from 2.63% to -1.48%, as shown in Fig. 16.

As the engine creep life consumption rate for the whole flight mission is assessed by the Equivalent Creep Factor (ECF), Fig. 17 shows how ECF for both the clean and the degraded engines change with the TBF of the clean engine at cruise flight condition. It can be seen that when TBF of the clean engine increases, ECF of the clean engine decreases while ECF of the degraded engine increases, indicating that the clean engine speeds up its creep life consumption while the degraded engine slow down its creep life consumption. When TBF of the clean engine reaches around 1.92, both engines reach the same ECF indicating that both engines consume creep life at the same rate.

Similarly, the thrust rebalancing also change the consumption of the effective number of flight cycles of the two engines. Fig. 18 shows that when TBF of the clean engine increases, the daily flight cycle consumption of the clean engine increases while the daily flight cycle consumption of the degraded engine decreases. At TBF of the clean engine being 1.92, the daily consumption of the effective numbers of flight cycles of the two engines become the same.

Fig. 19 shows the impact of TBF on the consumption of the flight cycles for both engines against the number of flight days. At the beginning of operation without applying the thrust rebalance method (TBF of clean engine = 0), the clean engine has 5,000 flight cycles available and therefore can fly 5,000 flight days. For the degraded engine, due to its degradation, it has higher creep life consumption rate and will run out of all the flight cycles on Day 2,460, as shown in Fig. 19. With the thrust rebalance method applied and the TBF

of the clean engine increases, the consumption of flight cycles of the clean engine will speed up and the number of flight days to consume all flight cycles will reduce. At the same time, the consumption of flight cycles for the degraded engine will slow down and the number of flight days to consume all flight cycles will increase. At the TBF being 1.92, both engines will consume all flight cycles on Day 3,410. In other words, the time on-wing for the degraded engine will be increased from 2,460 days to 3,410 days with the expenses of the clean engine having the time on-wing from 5,000 to 3,410 days. Consequently, the time between overhaul for the aircraft will be increased by 38.6% considering that the creep life of the degraded engine dominates the maintenance schedule. Therefore, the thrust rebalance method could enable the time on-wing for both the clean and the degraded engines expire at the same time and the time between overhaul of the aircraft could be maximized.

4 SENSITIVITY ANALYSIS

A sensitivity analysis has been carried out to look at the response of the key parameters to the change of the thrust balance factor. It is done by applying 1% increase in TBF of the clean engine and comparing the corresponding changes of the most important performance and life consumption parameters, such as net thrust, TET, PCN, ECF and daily flight cycle consumption.

As shown in Figure 20 at the cruise condition, an increase of TBF of the clean engine by 1% would result in 1% thrust rise of the clean engine and 1% thrust drop of the degraded engine in order to keep the total thrust generated by the two engines unchanged, as shown on Figure 20. Correspondingly, the clean engine would have to increase PCN by 0.25% and TET by 3.5K, while the degraded engine would be able to reduce PCN by 0.22% and TET by 4K,

For the whole flight mission, an increase of 1% of TBF of the clean engine would result in an increase of 1% of the net thrust, a drop of ECF by 53.15 and an increase of daily flight cycle consumption by 0.27 of the clean engine, while the degraded engine would have a drop of next thrust by 1%, an increase of ECF by 21.1 and a drop of daily flight cycle consumption by 0.296, as shown in Figure 21. It can be seen that the drop of TBF of the clean engine has slightly more positive effect on the daily flight cycle consumption of the degraded engine than the negative effect on that of the clean engine.

5 DISCUSSIONS

The thrust rebalance would bring both advantages and challenges to aircraft. For example, the asymmetric thrust would induce aircraft sideslip and therefore, the aircraft rudder must be used to maintain a straight flight path, which may result in increased structural stress. The auto pilot system must be modified to adapt such a thrust rebalance requirement. In addition, aircraft safety regulations may

be modified to accommodate such practice within safe limit. However, these issues are beyond the scope of this paper and need further research.

Gas turbine engines have also been widely used in power generation industry and marine propulsions. For these applications with multiple gas turbines installed, similar power re-balance concept may also be applied to control or extend time between overhaul (TBO) of gas turbine power plants when the level of degradations among the engines are different. This would bring significant benefits of improved plant availability and reduced maintenance costs.

6 CONCLUSIONS

This paper has introduced a novel thrust rebalance method for a twin-engine civil passenger aircraft with the aim to maximize the time between overhaul of the aircraft with the consideration of engine creep life consumption when one of the engines is degraded. The Equivalent Creep Factor (ECF) for a complete mission is used to assess the relative creep life consumption of the engines and the concept of Thrust Balance Factor (TBF) is introduced to optimize the amount of thrust shifted from the degraded engine to the clean engine. An iterative searching method is suggested to find the best value of the TBFs so the number of flight cycles for both engines could be run out at the same time. To demonstrate the application of the thrust rebalance method, two model engines similar to GE90-115B powering a model aircraft similar to Boeing 777-300ER flying between London and Toronto are used in this study. Based on the assumption that the initial flight cycles for the two engines is 5,000, one flight per day and one of the engines has a HP turbine degradation, the degraded engine may run out of its flight cycles in 2,460 flight days instead of 5,000 flight days. By applying the thrust rebalance method with TBF being 1.92, the degraded engine could extend its flight operation to 3,410 flight days with the expenses of a faster creep life consumption of the clean engine that could run out of its flight cycles from 5,000 flight days to 3,410 flight days. In other words, a 38.6% improvement in time between overhaul for the aircraft could be potentially achieved by applying the thrust rebalance method by extending the creep life of the degraded engine and shortening the creep life of the clean engine.

REFERENCES

- [1] Naeem M., Singh R., Probert D., "Implications of engine deterioration for creep life", *Applied Energy*, vol. 60, pp. 183-223, 8/1. 1998.
- [2] Naeem M., Singh R., Probert D., "Consequences of aero-engine deteriorations for military aircraft", *Applied Energy*, vol. 70, Issue 2, pp. 103-133, October 2001.

- [3] Naeem M., “Implications of day Temperature Variation for an Aero-engine’s HP Turbine-Blade's Creep Life-Consumption”, *Aerospace Science Technology*, vol. 13, pp. 27–35, 2009.
- [4] Tinga T., Visser W. P. J., Wolf, W. B., “Integrated lifing analysis for gas turbine components”, National Aerospace Laboratory, Amsterdam, Tech. Rep. NLR-TP-2000-632, 2000.
- [5] Liu Z., Mavris D., Volovoi V., “Creep life prediction of gas turbine components under varying operating conditions”, JPGC2001/PWR-19163, ASME International Joint Power Generation Conference, New Orleans, USA, June 2001.
- [6] Liu Z., Mavris D., Volovoi V., “Probabilistic remaining creep life assessment for gas turbine components under varying operating conditions”, AIAA-2002-1277, 43rd AIAA/ASME/ASCE/AHS/ASC Structures, Structural Dynamics, and Materials Conference, Denver, Colorado, USA, April 2002.
- [7] Wallace J., Wang R., Mavris D., “Creep life uncertainty assessment of a gas turbine airfoil”, AIAA-2003-1484, 44th AIAA/ASME/ASCE/AHS/ASC Structures, Structural Dynamics, and Materials Conference, Norfolk, Virginia, USA, April 2003.
- [8] Abdul Ghafir M. F., Li Y. G., Wang L., and Zhang W., “Impact Analysis of Aero-engine Performance Parameter Variation on Hot Section’s Creep Life Using Creep Factor Approach”, *AIAA Journal of Propulsion and Power*, vol. 16, no. 9, pp. 1–12, 2011.
- [9] Saturday E.G., Li Y.G. and Ogiriki E.A., “Creep life usage analysis and tracking for industrial gas turbines”, *AIAA Journal of Propulsion and Power*, Vol. 33, No. 5, pp 1305-1314, 2017.
- [10] James J. O’Dell P., “Derated Climb Performance in Large Civil Aircraft”, Article 6, Boeing Performance and Flight Operations Engineering Conference, 2005.
- [11] Atif Shafi, S., “Effect of Thrust Rating Change on Engine Time On-Wing”, PhD thesis, Cranfield University, 2014.
- [12] EASA, “Certification Specifications for Large Aeroplanes CS-25”, Amendment 3, 19 September 2007.
- [13] Macmillan W. L., “Development of a Modular Type Computer Program for the Calculation of Gas Turbine Off Design Performance”, Ph.D. Thesis, Cranfield University, September 1974.
- [14] Li Y. G. and Singh R., “An Advanced Gas Turbine Gas Path Diagnostic System-PYTHIA”, ISABE-2005-1284, The XVII International Symposium on Air Breathing Engines, Munich, Germany, 2005.
- [15] Alozie O., Li Y. G., Diakostefanis M., Wu X., Shong X. and Ren W., “Assessment of Degradation Equivalent Operating Time for Aircraft Gas Turbine Engines”, *Aeronautical Journal*, Vol. 124, Issue 1274, pp. 549-580, April 2020.
- [16] Vaezi M., Soleymani M., “Creep Life Prediction of Inconel 738 Gas Turbine Blade”, *Journal of Applied Sciences*, vol. 9, no. 10, pp. 1950–1955, 2009.

- [17] Marahleh G., Kheder A. R. I., and Hamad H. F., “Creep-Life Prediction of Service-Exposed Turbine Blades”, *Materials Science*, vol. 42, no. 4, pp. 476–481, July 2006.
- [18] Kong Z. and Li S., “Effects of Temperature and Stress on the Creep Behavior of a Ni 3 Al Base Single Crystal Alloy”, *Progress in Natural Science: Materials International*, vol. 23, no. 2, pp. 205–210, 2013.
- [19] Daly, M., *GE-90 in Jane’s Aero Engines*, pp. 535–543, 2017.

APPENDIX A – TBF OF DEGRADED ENGINE

At $\lambda_c = 0$, the clean engine has the baseline net thrust of $NT_{c,bl}$ and the degraded engine has the baseline net thrust of $NT_{d,bl}$. $NT_{d,bl}$ is obtained by keeping the handle parameter of the degraded engine the same as that of the clean engine. When the thrust rebalance is applied as shown in Fig. A, the net thrust of the clean engine is

$$NT_c = NT_{c,bl} * (1 + \lambda_c) \quad (A-1)$$

And the net thrust of the degraded engine is

$$NT_d = NT_{c,bl} * (1 - \lambda_c) \quad (A-2)$$

The thrust rebalance factor for the degraded engine can be calculated by Eq. (A1-3)

$$\lambda_d = \frac{NT_d - NT_{d,bl}}{NT_{d,bl}} = \frac{NT_{c,bl} * (1 - \lambda_c) - NT_{d,bl}}{NT_{d,bl}} \quad (A-3)$$

Therefore,

$$\lambda_d = \frac{NT_{c,bl}}{NT_{d,bl}} * (1 - \lambda_c) - 1 \quad (A-4)$$

Tables

Table 1. Performance specification of model engine at 15 °C at ISA sea level static condition

| Parameters | Unit | Value |
|---------------------------|-------------|--------------|
| Thrust | kN | 516 |
| SFC | g/kN-s | 8.9 |
| Overall Pressure Ratio | | 42 |
| Turbine entry temperature | K | 1,730 |
| Air mass flow rate | kg/s | 1,641 |
| Bypass ratio | | 7.1 |
| Fan pressure ratio | | 1.58 |

Figures

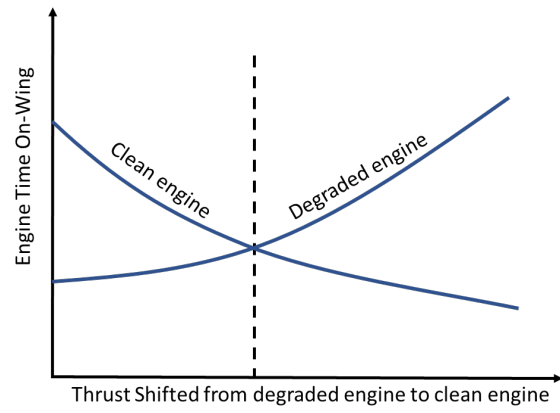
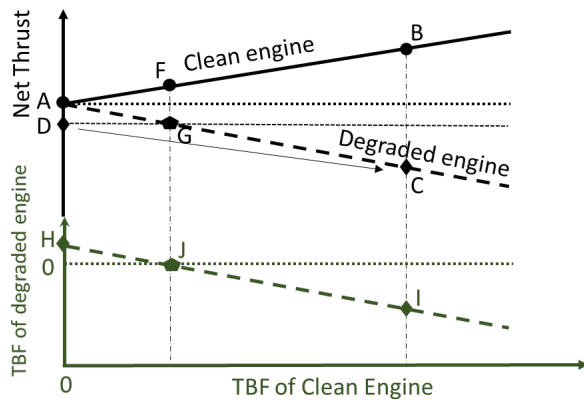
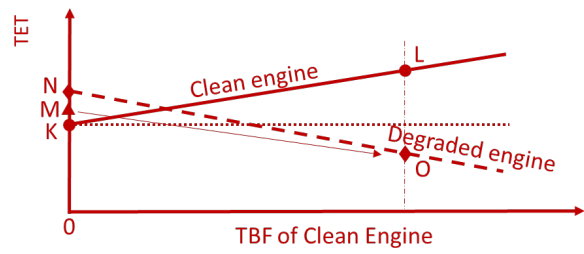


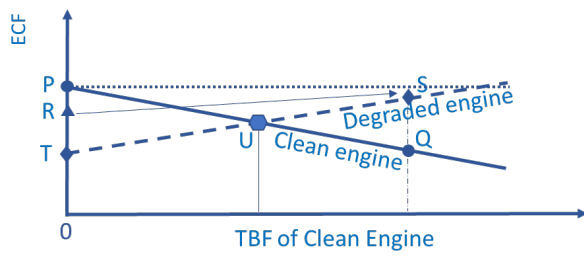
Figure 1: Engine Thrust Rebalance Strategy



(a) Net Thrust vs TBF



(b) TET vs TBF



(c) ECF vs TBF

Figure 2: Impact of Thrust Rebalance

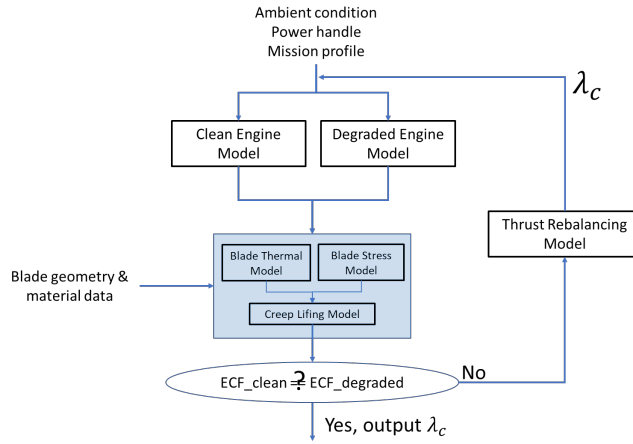


Figure 3: Flow chart of thrust rebalance method

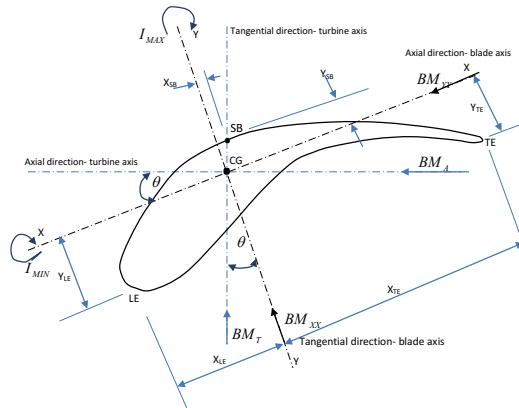


Figure 4 Bending moments in a turbine blade [9]

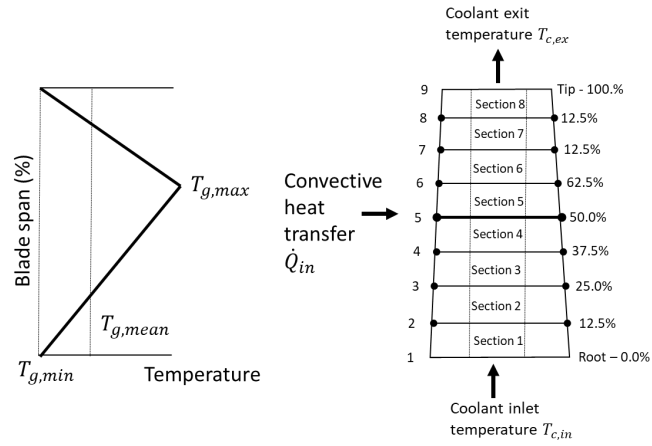


Figure 5 Gas and blade temperature distribution [9]

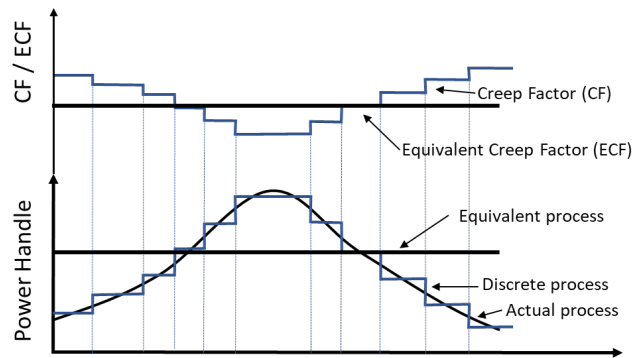


Figure 6 Actual and Equivalent Operation Processes [9]

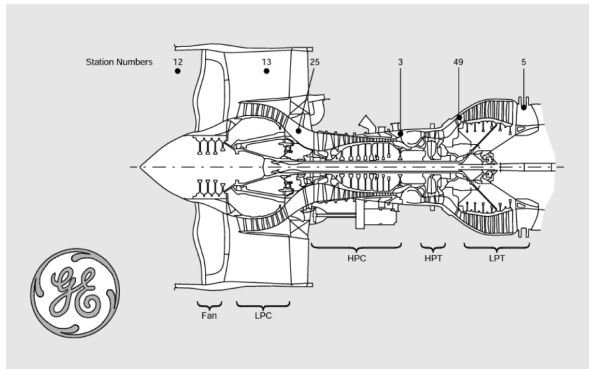


Figure 7: GE90-115B [18]

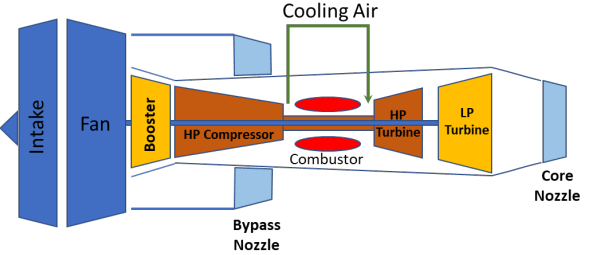


Figure 8 Engine model layout with station identification

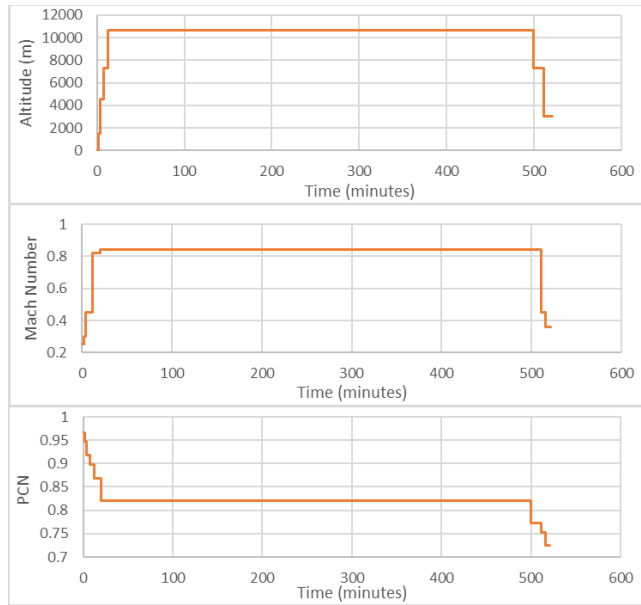


Figure 9. Flight mission profile

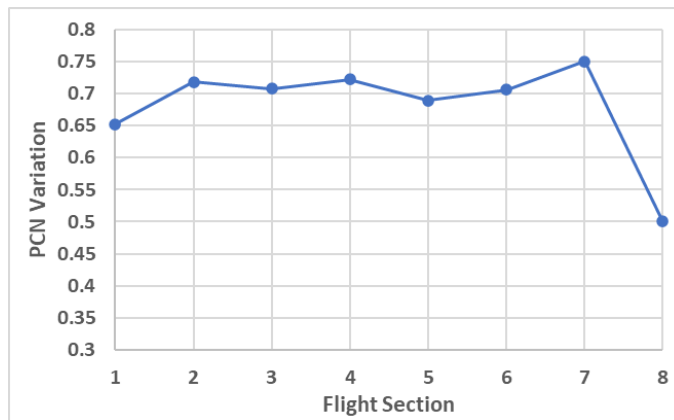


Figure 10: PCN variation of degraded engine against clean engine (TBF = 0)

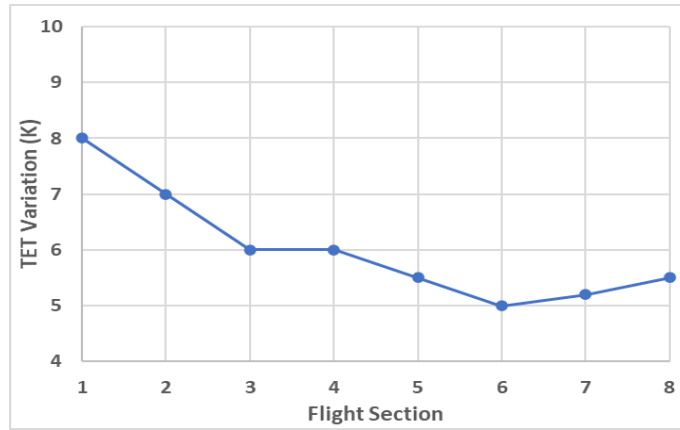
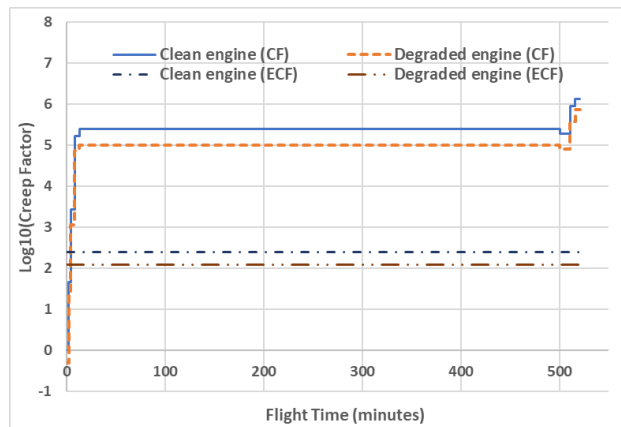
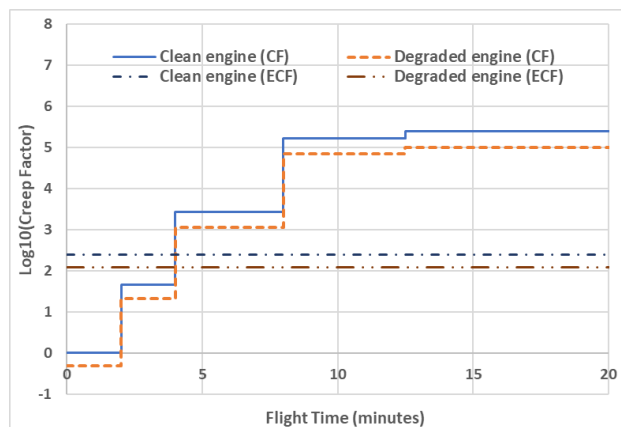


Figure 11 TET variation of degraded engine against clean engine (TBF = 0)



(a)



(b)

Figure 12 Creep Factors of both engines (TBF = 0)

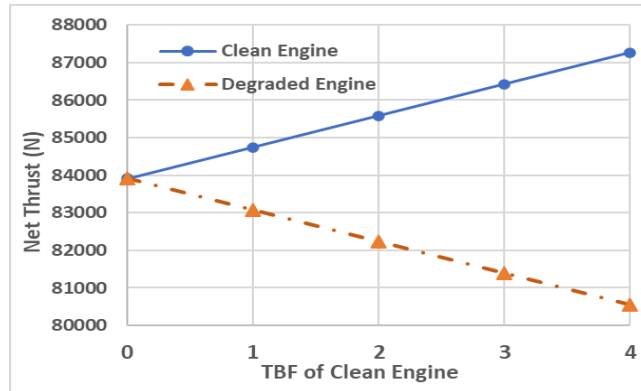


Figure 13: Net thrust vs TBF at cruise condition

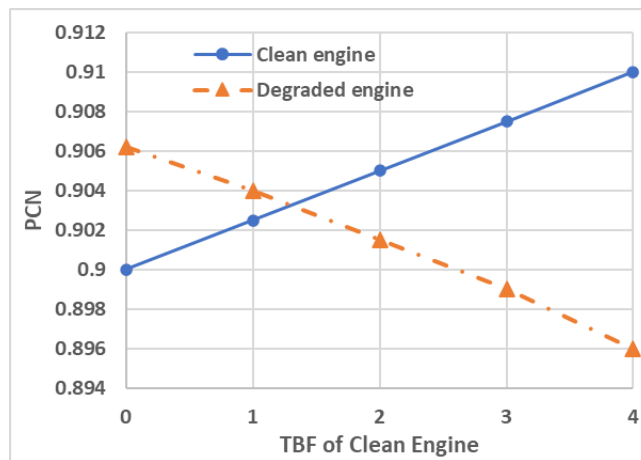


Figure 14: PCN vs TBF at cruise condition

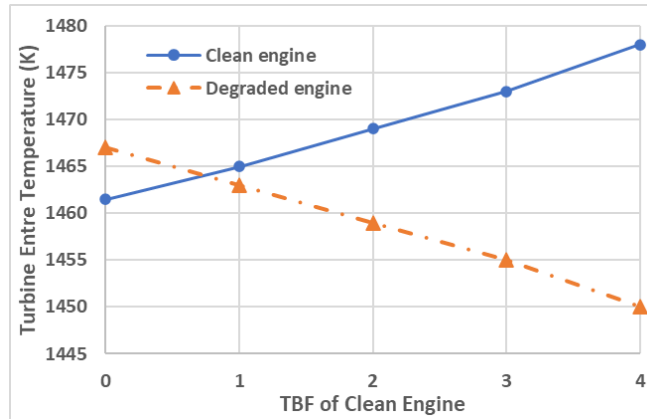


Figure 15: TET vs TBF at cruise condition

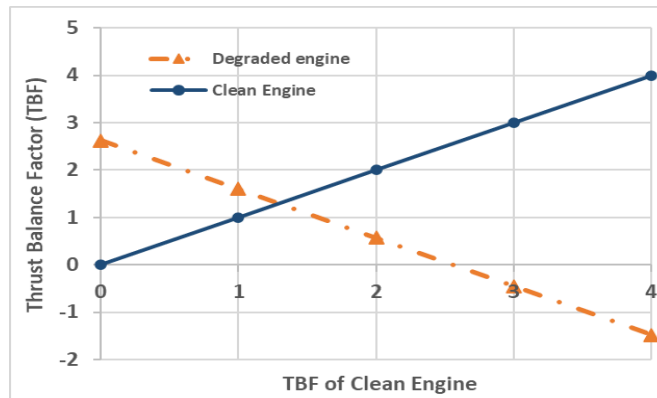


Figure 16: TBF of both engines at cruise condition

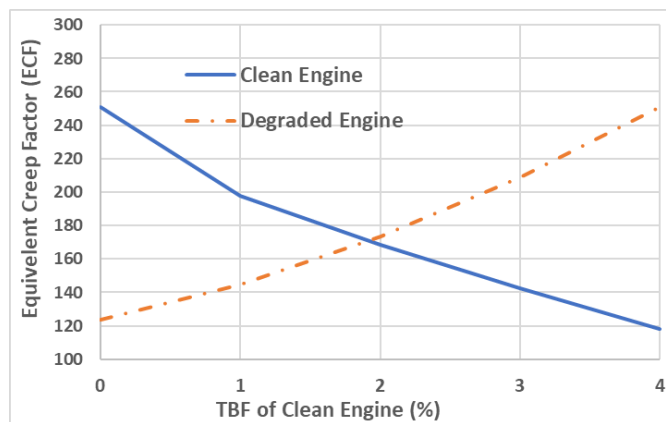


Figure 17: ECF vs TBF at cruise condition

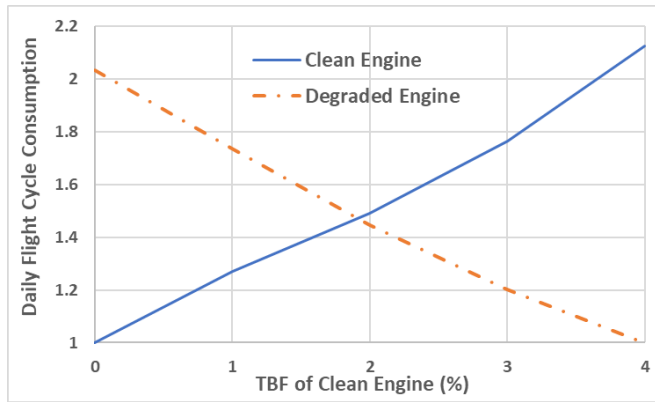


Figure 18 Daily flight cycle consumption vs TBF

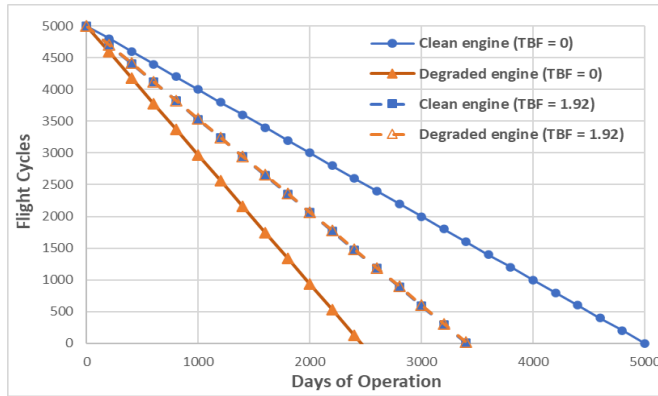


Figure 19: Flight cycle consumption

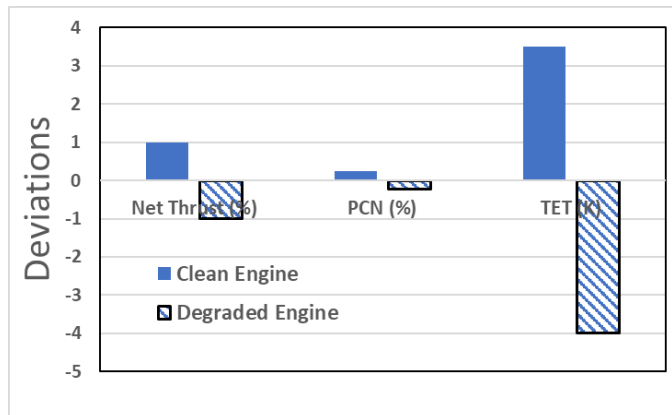


Figure 20: Sensitivity of PCN & TET to 1% change of TBF of clean engine at cruise condition

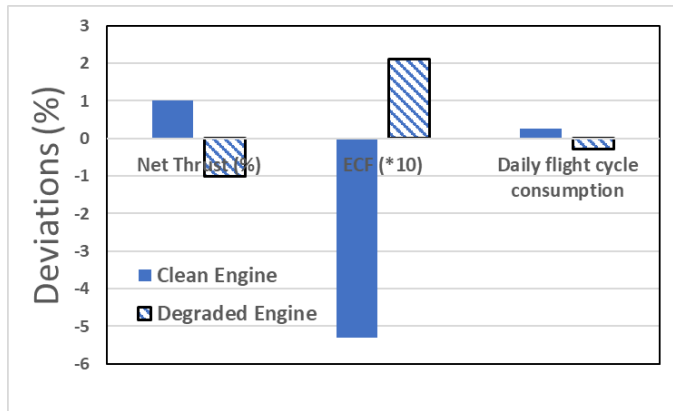


Figure 21: Sensitivity of ECF & daily flight cycle consumption to 1% change of TBF of clean engine of whole flight mission

List of Table Captions

Table 1. Performance specification of model engine at 15°C at ISA sea level static condition

List of Figure Captions

Figure 1: Engine Thrust Rebalance Strategy

Figure 2: Impact of Thrust Rebalance

Figure 3: Flow chart of thrust rebalance method

Figure 4 Bending moments in a turbine blade [9]

Figure 5 Gas and blade temperature distribution [9]

Figure 6 Actual and Equivalent Operation Processes [9]

Figure 7: GE90-115B [18]

Figure 8 Engine model layout with station identification

Figure 9. Flight mission profile

Figure 10: PCN variation of degraded engine against clean engine (TBF = 0)

Figure 11 TET variation of degraded engine against clean engine (TBF = 0)

Figure 12 Creep Factors of both engines (TBF = 0)

Figure 13: Net thrust vs TBF at cruise condition

Figure 14: PCN vs TBF at cruise condition

Figure 15: TET vs TBF at cruise condition

Figure 16: TBF of both engines at cruise condition

Figure 17: ECF vs TBF at cruise condition

Figure 18 Daily flight cycle consumption vs TBF

Figure 19: Flight cycle consumption

Figure 20: Sensitivity of PCN & TET to 1% change of TBF of clean engine at cruise condition

Figure 21: Sensitivity of ECF & daily flight cycle consumption to 1% change of TBF of clean engine of whole flight mission

2023-10-18

Thrust rebalance to extend engine time on-wing with consideration of engine degradation and creep life consumption

da Mota Chiavegatto, Rafael

American Society of Mechanical Engineers

da Mota Chiavegatto R, Li Y-G. (2023) Thrust rebalance to extend engine time on-wing with consideration of engine degradation and creep life consumption. *Journal of Engineering for Gas Turbines and Power*, Volume 146, Issue 9, September 2024, Article number 091006, Paper number GTP-23-1576

<https://doi.org/10.1115/1.4063791>

Downloaded from Cranfield Library Services E-Repository